Coordinated Control of DC Circuit Breakers in Multilink HVDC Grids

Xibei Zhao, *Member*, *IEEE*, *Member*, *CSEE*, Jianzhong Xu, *Senior Member*, *IEEE*, *Member*, *CSEE*, Gen Li, *Member*, *IEEE*, *Member*, *CSEE*, Jinsha Yuan, and Jun Liang, *Senior Member*, *IEEE*, *Member*, *CSEE*

***Abstract*—High voltage DC grids are developing in more terminals and with larger transmission capacity, thus the requirements for DC circuit breakers (DCCB) will continue to rise. Conventional methods only use the faulty line DCCB to withstand the fault stress, and therefore this paper presents a coordination method of multiple DCCBs to protect the system. As many adjacent DCCBs are tripped to interrupt the fault current, the fault energy is shared, and the requirement for the faulty line DCCB is reduced. Moreover, the adjacent DCCBs are actively controlled to help system recovery. The primary protection, backup protection, and reclosing logic of multiple DCCBs are studied. Simulations confirm that the proposed control reduces the energy dissipation requirement of faulty line DCCB by approximately 30%–42%, the required current rating for IGBTs is reduced, and the system recovery time is also reduced by 20–40 ms.**

***Index Terms*—DC circuit breakers (DCCB), DC fault, DC grid, DC protection, fault current limiting.**

I. Introduction

HIGH voltage DC grids are a promising solution for large-scale renewable energy transmission and regional AC grid interconnections. A multilink DC grid is built with several transmission lines linked to one DC bus, which can improve functionality, stability, and reliability of the power grid while decreasing the investment cost of many two-terminal DC projects [1], [2]. DC grids are characterized by low impedance, and thus, a significant challenge of the DC grid is the fast propagation of the DC fault [3], [4]. However, a multilink of transmission lines will further aggravate this condition.

To meet the requirements of DC grid protection, the fault current should be interrupted within a few milliseconds. A hybrid DC circuit breaker (DCCB), which can achieve low power loss and fast fault interruption at the same time, is considered an effective solution for DC grid protection. The DCCB has better technical performance as it only isolates the faulty line, but other converter-based fault interruption methods need the near-fault converter to participate in the fault clearing. Therefore, the fault area expands [5]–[9]. The concept of hybrid DCCB is proposed in [10] and verified by a prototype with 10 kA/2 ms fault interruption capability. State Grid Cooperation of China installed the first practical installation of a hybrid DCCB in the Zhoushan 200 kV five-terminal DC project with a 15 kA/3 ms interruption capacity [11]. In 2020, the 25 kA/3 ms hybrid DCCB will be used in the Zhangbei 500 kV DC grid [12].

As one of their disadvantages, hybrid DCCBs will increase the investment and operational costs when a large number of DCCBs are installed at each terminal along all the transmission lines in a multilink DC grid. To address this issue, one feasible approach is to reduce the cost of individual DCCBs, and simplified topologies and improved control algorithms are proposed [13]. A diode bridge-type rectifier is used to regulate bidirectional current to unidirectional current, thus there is no need for IGBT units with bidirectional fault-blocking capability [14], [15]. Using some auxiliary capacitors, the Thyristors can be used to replace the IGBTs, creating cheaper prices [16], [17]. By sequential triggering subunits within hybrid DCCB, the peak fault current and energy dissipation are reduced by an earlier blocking of the subunits [18], [19], thereby increasing the controllability of the hybrid DCCB topologies.

Another approach is to reduce the required number of DCCBs. In this category, an integrated DCCB can be installed at each DC bus rather than using several line-side DCCBs [20]. The integrated DCCB will share the use of the semiconductor devices, creating the need for a specially designed circuit to ensure that the fault current from any direction flows into the forward direction of the IGBTs [21], [22]. In [23], each normal current branch of the DCCB is switched off to act as a rectifier, and the remaining branch will commutate the fault current to the IGBTs.

The above two approaches both use one DCCB to deal with one primary protection, and the individual DCCBs have the benefit of simple fault interruption logic, while the integrated DCCBs cost less due to the reduced installation number. However, the fault voltage and current stresses will be fully imposed on the one integrated or individual DCCB, and the stresses will rise when the links connected to the same bus increase.

In this study, a coordination method of multiple DCCBs to protect one faulty line is proposed. Since the fault energy

Manuscript received September 23, 2020; revised December 7, 2020; accepted February 3, 2021. Date of online publication November 9, 2021; date of current version November 2, 2023. This work was supported by the National Key R&D Program of China (Grant No. 2018YFB0904600) and the National Natural Science Foundation of China (Grant No. 51777072).

X. B. Zhao, J. Z. Xu (corresponding author, email: xujianzhong@ncepu.edu.cn), and J. S. Yuan are with the State Key Laboratory of Alternate Electrical Power System with Renewable Energy Sources, North China Electric Power University, Beijing 100096, China.

G. Li is with the Technical University of Denmark, Denmark.

J. Liang is with the School of Engineering, Cardiff University, UK.

DOI: 10.17775/CSEEJPES.2020.05170

feeding from the adjacent lines will rise in the multilink DC grid, the DCCBs in adjacent lines also participate in the protection of the faulty line. Thus, the fault energy is shared by multiple DCCBs, and the requirement for a faulty line DCCB will be reduced. Moreover, by using the current-limiting control DCCB, the current on the adjacent lines is actively controlled, which can help to accelerate the power recovery process of the DC grid.

Compared to the existing approach of one DCCB installed on one line, the proposed method can be used to upgrade the protection performance of the existing grid. Compared to the integrated DCCB, the proposed scheme doesn't rely on a complex current commutation process during the fault, and the backup protection can still be achieved by the adjacent DCCBs.

Following this Introduction, the control modes of DCCB are introduced in Section II. The coordination control for the multiple DCCBs on different lines is proposed in Section III, which considers primary/backup protection, fault reclosing and fast recovery. In Section IV, the proposed method is validated in a HVDC grid simulation. Comparisons and discussions are given in Section V, and Section VI concludes this paper.

II. The Control Modes of DCCB

The conventional control of DCCB synchronously switches all IGBT units of its main breaker (MB). In contrast, the sequential blocking control and current limiting control of the DCCB separately switches its MB IGBT units. A test circuit of the 500 kV/2 kA hybrid DCCB model is shown in Fig. 1 to illustrate the DCCB's performance under three control modes.

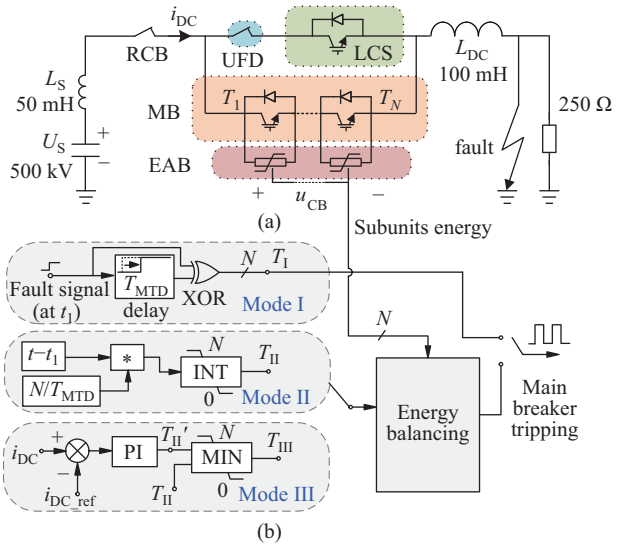

Fig. 1. DCCB text scheme. (a) Test circuit. (b) DCCB control modes.

In Fig. 1, U_S and L_S represent the converter system DC voltage and its equivalent inductance. L_{DC} represents the lineside DC inductance, and RCB represents the residual circuit breaker. The DCCB consists of an ultra-fast disconnector (UFD), a load commutation switch (LCS), a main breaker (MB) with N ($N = 8$) subunits, and an energy absorption branch (EAB) build up with metal-oxide varistors. The three different control strategies of the main breaker are shown in Fig. 1(b):

1) Mode I (conventional DCCB): All the MB subunits share the same triggering signal T_I. They will be conducted after receiving the fault signal at t_1 and blocked when the UFD successfully separates after the mechanical time delay (T_{MTD}). This is achieved by XORing the step fault signal and its delay.

2) Mode II (sequential blocking DCCB) [18], [19]: T_{II} is the number of blocked subunits, which is calculated by evaluating the contact insulation voltage of the UFD, and then it rounds down through the limiter. In this mode, a proportion of the subunits are blocked sequentially during the UFD separation, and all the subunits are blocked after the UFD is fully opened at t_2.

3) Mode III (sequential current-limiting DCCB) [24]: A current feedback control is employed to control the DC current by changing the number of inserted varistors, where i_{DC_ref} is the reference DC current and i_{DC} is the real-time measured current. Signal T_{II} is used to limit the blocked number of subunits during the UFD separation, and T_{II}' is the required number of subunits generated from the current controller. Finally, the number of blocked subunits T_{III} is determined by the minimum value of T_{II} and T_{II}'.

An energy balancing module is used in Modes II and III to ensure that all the subunits equally share in the fault energy [24], and the control frequency is 10 kHz [19]. The dissipated energy of each subunit is calculated by its corresponding sensor, and the energy balancing module determines which x subunits with the lowest energy are blocked.

Among the three modes, Mode I is the very basic control of DCCB, which considers all subunits as an entity, and the control signal comes from an open loop signal. Mode II can control each subunit independently, but T_{II} also comes from an open loop. Mode III further adopts close-loop control, so it has the highest flexibility. Moreover, Modes II and III can be seen as a Mode I step-by-step upgrade through software and hardware. The DCCB's performance for the three modes is shown in Fig. 2.

The fault is applied at t_0 and detected at t_1. As shown in

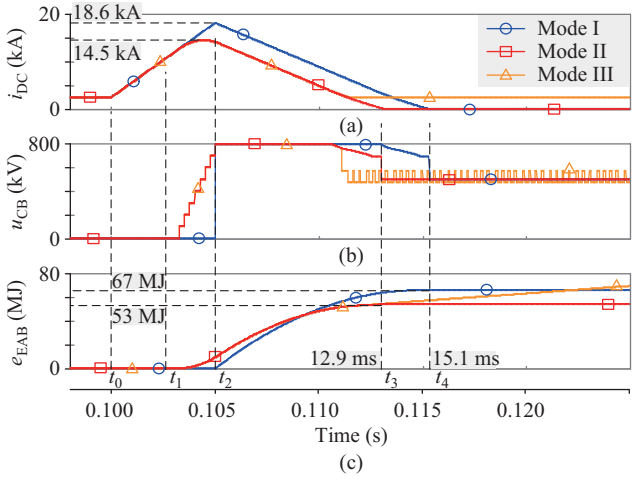

Fig. 2. DCCB performance. (a) DC current. (b) DC breaker voltage. (c) Energy dissipated in the EAB.

Fig. 2(a), the peak current of Mode I is 18.6 kA, while the peak current of Modes II and III are reduced to 14.5 kA. It is seen from Fig. 2(b) that the breaker voltage of Mode I is established after UFD is fully opened at t_2, but Modes II and III can partly insert subunits during UFD separation. Moreover, the energy dissipation is reduced from 67 MJ to 53 MJ due to the earlier blocking of subunits in Mode II, see Fig. 2(c). Mode III has the same response as Mode II in the beginning. Then the subunits are controlled on/off to follow the $i_{\mathrm{DC\_ref}}$ ($=2$ kA). Note that the energy dissipation in Mode III will continuously increase, which indicates that the dissipated energy will increase if Mode III is applied to the faulty line DCCB. However, it can be applied to the adjacent DCCBs as their fault energy is lower than the faulty line. Based on the different control modes, the coordination methods between DCCBs can be discussed.

III. Coordination Method of DCCBs in DC Grid

In this section, the coordination methods of Modes II and III are investigated, in which the primary/backup protection, fault reclosing and fast recovery are considered.

A. Coordination Method for Primary Protection

The sequential blocking of the DCCB can reduce the peak fault current and fault energy by independently controlling each subunit, and the dissipation energy can be reduced by the coordination control at the same time. The schematic diagram of the proposed coordination method is shown in Fig. 3. Here, a three-link DC bus is assumed, and the MMC0 is the converter directly connected to the faulty line. MMC1&2 are remote converters feeding fault currents through DC lines.

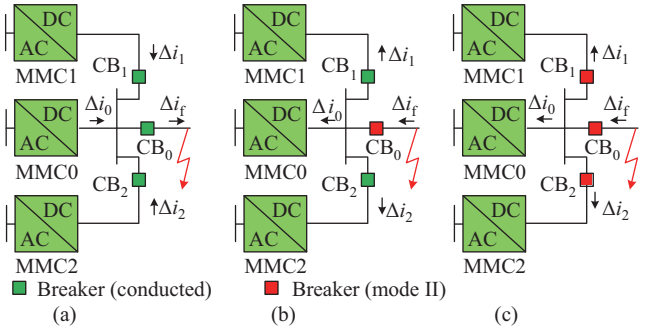

Fig. 3. Coordination method for sequential blocking DCCBs. (a) Current trend after fault. (b) Conventional protection. (c) Proposed coordination protection.

After the fault occurs, all the converters in the DC grid have a trend to feed the fault current into the fault point. As shown in Fig. 3(a), the current from the MMC0 will be the main part of the total fault current because it has less inductance on the fault path, while the proportion will decrease with more DC links. However, the peak fault current will increase with more DC links, and the energy dissipation requirements of the DCCBs will increase faster since more inductive energies stored in the DC links have to be dissipated (this will be validated later in Section IV).

The conventional protection only uses one CB_0 (Mode II) to interrupt the fault current, and the current on the adjacent lines will decrease naturally to achieve a new steady state, see Fig. 3(b). To reduce the requirement of faulty line CBs, the breakers installed on the adjacent lines ($\mathrm{CB}_{1\&2}$) can also be tripped (Mode II) to help CB_0, see Fig. 3(c). As all corresponding CBs are in the same station, they are supposed to operate simultaneously. The adjacent CBs are designed to deal with their line fault, but the adjacent lines' currents are much smaller than the faulty line's current. Therefore, the adjacent DCCBs can easily interrupt their currents.

The equivalent circuit of the DC grid fault shown in Fig. 4 is used to analyze the fault interruption performance, where all the adjacent and remote terminals are considered as constant DC voltage sources. In Fig. 4, U_{S} and L_{S} represent the converter DC voltage and its equivalent inductance. L_{DC} represents the DC inductance, in which the label 0 means the elements on the faulty line and the directly linked converter, and the label $1 \sim n$ means elements on the n adjacent lines.

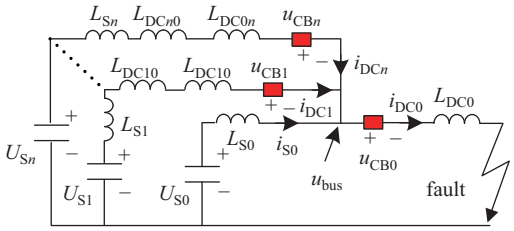

Fig. 4. Equivalent circuit for a DC grid fault.

When a DC solid fault occurs at t_0, it is detected at t_1 before the breaker is tripped at t_2, then the DC bus voltage u_{bus} is:

$$u_{\mathrm{bus}} = L_{\mathrm{DC0}}\frac{\mathrm{d}i_{\mathrm{f}}}{\mathrm{d}t} = U_{\mathrm{S}\beta} - L_{\mathrm{eq}\beta}\frac{\mathrm{d}i_{\beta}}{\mathrm{d}t},\ \beta \in \{0, n\} \tag{1}$$

where the subscript β is $\{0, 1, 2, \cdots, n\}$ to represent the DC lines and corresponding converters. $L_{\mathrm{eq}\beta}$ is the equivalent inductance of each line given in (2)

$$\begin{cases} L_{\mathrm{eq}\beta} = L_{\mathrm{S0}}, & \beta = 0 \\ L_{\mathrm{eq}\beta} = L_{\mathrm{S}\beta} + L_{\mathrm{DC}\beta 0} + L_{\mathrm{DC0}\beta}, & \beta = 1, 2, \cdots, n \end{cases} \tag{2}$$

The fault current will reach its maximum value if all converters can be considered to keep at the rated DC voltage (U_{S}) for a short time. Thus, the DC fault current on each line is:

$$\begin{cases} i_{\mathrm{f}} = i_{\mathrm{f}(t_0)} + \dfrac{U_{\mathrm{S}}}{L_{\mathrm{DC0}} + L_{\mathrm{eq}}}t \\ i_{\beta} = i_{\beta(t_0)} + \dfrac{L_{\mathrm{eq}}}{L_{\mathrm{eq}\beta}}\dfrac{U_{\mathrm{S}}}{L_{\mathrm{DC0}} + L_{\mathrm{eq}}}t \\ \dfrac{1}{L_{\mathrm{eq}}} = \sum \dfrac{1}{L_{\mathrm{eq}\beta}} \\ t \in (t_0, t_2),\ \beta \in \{0, 1, \cdots, n\} \end{cases} \tag{3}$$

The L_{eq} will become smaller with more DC links, and the rising speed of i_{f} will increase, but it will have a maximum value when L_{eq} equals zero. The rising rate of i_{β} is inversely proportional to the value of $L_{\mathrm{eq}\beta}$.

If one DCCB based on sequential control is used to interrupt the faulty line, the subunits of DCCB are blocked during the UFD separation process. Before the UFD is fully separated, the $u_{\rm CB}$ can be seen to follow the isolation voltage of UFD. After the UFD is fully separated, the CB's voltage will reach its rating voltage $U_{\rm CB}$ [15]. Thus, the voltage across the DCCB is:

$$u_{\rm CB} = \begin{cases} K \times t, & t \in (t_1, t_2) \\ U_{\rm CB}, & t \in (t_2, t_3) \end{cases} \tag{4}$$

During t_1–t_2, the fault current changes with the growth of $u_{\rm CB}$:

$$\begin{aligned} i_{\rm f} &= i_{\rm f}(t_1) + \int_{t_1}^{t} \frac{U_{\rm S} - u_{\rm CB}}{L_{\rm DC0} + L_{\rm eq}} {\rm d}t \\ &= i_{\rm f}(t_1) + \frac{U_{\rm S}(t - t_1) - 0.5K(t - t_1)^2}{L_{\rm DC0} + L_{\rm eq}},\ t \in (t_1, t_2) \end{aligned} \tag{5}$$

Due to the earlier blocking of subunits by the conventional DCCB, the peak fault current is limited, and the fault current will achieve its maximum value when the breaker voltage equals the DC system voltage.

$$i_{\rm f\_peak} = i_{\rm f}(t_1) + \frac{U_{\rm S}\frac{U_{\rm CB}}{K} - 0.5K\left(\frac{U_{\rm CB}}{K}\right)^2}{L_{\rm DC0} + L_{\rm eq}} \tag{6}$$

After all the subunits are blocked at t_2, the fault current decreases as:

$$i_{\rm f} = i_{\rm f}(t_2) + \frac{U_{\rm S} - u_{\rm CB0}}{L_{\rm DC0} + L_{\rm eq}} t,\ t \in (t_2, t_3) \tag{7}$$

The dissipation energy is the sum energy during t_1–t_3:

$$\begin{aligned} E_{\rm CB} &= \int_{t_1}^{t_2} i_{{\rm f}(t_2 - t_1)} K t {\rm d}t + \int_{t_2}^{t_3} i_{{\rm f}(t_3 - t_2)} U_{\rm CB} {\rm d}t \\ &= 0.5 i_{{\rm f}(t_1)} K (t_2 - t_1)^2 \\ &\quad + \frac{\frac{1}{3}U_{\rm S}K(t_2 - t_1)^3 - \frac{1}{8}k^2(t_2 - t_1)^4}{L_{\rm DC0} + L_{\rm eq}} \\ &\quad + U_{\rm CB} i^2_{{\rm f}(t_2)} \frac{L_{\rm DC0} + L_{\rm eq}}{2(U_{\rm CB} - U_{\rm S})} \end{aligned} \tag{8}$$

The proposed coordination method of multiple DCCBs will bring new characteristics if multiple DCCBs are used to interrupt the fault. The faulty line current will be reduced faster due to the participation of the adjacent DCCBs. Assuming all the DCCBs are tripped, the DCCBs on the adjacent lines will also be tripped to accelerate the fault current decay speed. The DC bus voltage is:

$$\begin{aligned} u_{\rm bus} &= L_{\rm DC0}\frac{{\rm d}i_{\rm f}}{{\rm d}t} + u_{\rm CB0} = U_{\rm S} - L_{{\rm eq}\beta}\frac{{\rm d}i_{\beta}}{{\rm d}t} - u_{{\rm CB}\beta} \\ &= U_{\rm S} - L_{\rm S0}\frac{{\rm d}i_0}{{\rm d}t},\ \beta \in \{1, 2, \cdots, n\} \end{aligned} \tag{9}$$

Because each DCCB will simultaneously block its subunits, the fault current under the coordination method of Mode II is:

$$\begin{aligned} i_{\rm f} &= i_{\rm f}(t_1) + \int_{t_1}^{t} \frac{U_{\rm S} - \frac{(2n+1)}{n+1}Kt}{\left(L_{\rm DC0} + \frac{1}{n+1}L_{\rm eq}\right)} {\rm d}t \\ &= i_{\rm f}(t_1) + \frac{U_{\rm S}t - 0.5\frac{(2n+1)}{n+1}Kt^2}{\left(L_{\rm DC0} + \frac{1}{n+1}L_{\rm eq}\right)},\ t \in (t_1, t_2) \end{aligned} \tag{10}$$

Equation (10) shows that the decay speed of the fault current will be faster with more adjacent DCCBs participating in the fault interruption process. Furthermore, the energy dissipation on the faulty line DCCB is reduced due to a faster fault current decay speed. The peak fault current is also reduced to:

$$i_{\rm f\_peak} = i_{\rm f}(t_1) + \frac{U_{\rm S}\frac{U_{\rm CB}}{K} - 0.5\frac{(2n+1)}{n+1}K\left(\frac{U_{\rm CB}}{K}\right)^2}{\left(L_{\rm DC0} + \frac{1}{n+1}L_{\rm eq}\right)} \tag{11}$$

The energy dissipation requirement for the faulty line DCCB can be calculated as:

$$\begin{aligned} E_{\rm CB} &= 0.5 i_{\rm f}(t_1) \times K(t_2 - t_1)^2 \\ &\quad + \frac{\frac{1}{3}U_{\rm S}K(t_2 - t_1)^3 - \frac{1}{8}\frac{2n+1}{n+1}K^2(t_2 - t_1)^4}{L_{\rm DC0} + \frac{1}{n+1}L_{\rm eq}} \\ &\quad + U_{\rm CB} \times i^2_{\rm f}(t_2) \times \frac{L_{\rm DC0} + L_{\rm eq}}{2\frac{2n+1}{n+1}(U_{\rm CB} - U_{\rm S})} \end{aligned} \tag{12}$$

Comparing (12) to (8), the second and third part of (12) becomes smaller with the growth of n. Therefore, the faulty line DCCB energy dissipation is reduced. Note that if no adjacent lines exist ($n = 0$), (10) and (12) are the same as (5) and (8), respectively.

Although the breaking of all adjacent DCCBs can help with the maximum share of the fault energy from $\rm CB_0$, a total breaking will damage the DC grid connection. Therefore, $\rm CB_{1\&2}$ is designed to operate in the current limiting mode to balance the energy sharing and system connection requirements.

B. Coordination Method for Assisting the System Fast Recovery and Backup Protection

The sequential current limiting DCCB (Mode III) can be applied to the adjacent lines. It is known that the fast system recovery is also important for the HVDC grid after the fault clearance, and the sequential current limiting DCCB can also contribute to this process in two ways:

1) Demagnetize the adjacent lines: As the fault current is much higher than the steady-state current, the adjacent DCCB action can assist current decreasing in the proposed coordination method. The excess line reactor energy is demagnetized by the DCCBs, so that the current of adjacent lines is actively reduced to a steady state value. However, this is not the case for the single DCCB protection since its power flow can only be established naturally.

2) Limit the current fluctuation during the recovery process: The $\rm CB_{1\&2}$ operates in Mode III, so the circuit breaker will not limit its current over the post-fault steady current. The $i_{\rm DC\_ref}$ of the current limiting mode can be obtained from the steady state power flow calculation [25], then the system fluctuation is forcibly suppressed by the circuit breaker. As shown in Fig. 5(a), the $\rm CB_0$ operates in Mode II, and $\rm CB_{1\&2}$ operates in Mode III. After the system recovers, the $\rm CB_{1\&2}$ will switch to the pre-fault state.

Based on the proposed primary protection method, the backup protection of multiple DCCBs is different from the conventional scheme. The conventional backup protection will only be tripped after receiving the fault signal of the faulty line

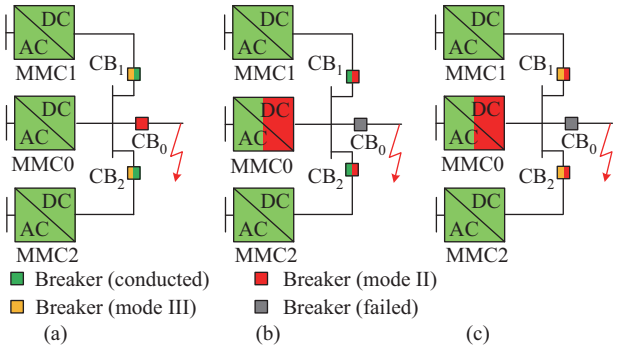

Fig. 5. Coordination method for (a) fast recovery; (b) conventional backup protection; (c) the proposed backup protection.

DCCB, then the near-fault converter (MMC0) and adjacent DCCBs ($CB_{1\&2}$) are blocked, as shown in Fig. 5(b). The backup protection of coordination control shows only a little difference from the main protection. All the breakers will switch to Mode II after receiving the signal of CB_0, and the near-fault converter will be blocked at the same time, see Fig. 5(c). The converter will not be blocked, and only the faulty line will be isolated if the DCCBs operate successfully, so no converter is lost in the proposed method, which is critical for fully selective protection. Although the adjacent DCCBs are activated, they are used to actively help the power flow rebalance. Therefore, the selectivity of the proposed method is still guaranteed.

The sequence of the proposed coordination control is shown in Fig. 6. The CB_0 is blocked to isolate the faulty line once the fault is detected. $CB_{1\&2}$ is used to regulate the currents in the adjacent lines within the threshold. If CB_0 fails, the system will switch to the backup protection. Then, MMC0 and $CB_{1\&2}$ will be blocked. The difference between the proposed method and conventional DCCB protection is highlighted in grey in Fig. 6, which shows the adjacent DCCBs (CB_1 and CB_2) will operate in the current-limiting mode to limit the adjacent lines' current fluctuation. As the proposed coordination method only has one additional operation, its complexity is only slightly increased with acceptable reliability and feasibility.

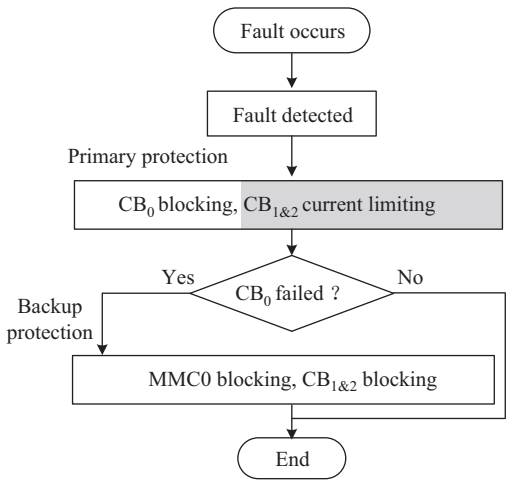

Fig. 6. Control logic of the coordination method of multiple DCCBs.

The converter will not change its state if the DCCB operates properly. Thus the protection is achieved by the DCCBs. If the faulty line DCCB fails, the converter will also be blocked, but it will only happen in the backup protection. The coordination control of backup protection has no difference at the beginning of primary protection. Thus no time delay occurs waiting for the failure signal of CB_0. Therefore, the proposed backup protection will act faster than the conventional method. Furthermore, this coordination method blurs the differences between the primary and backup protections, and the system only needs first to trip all DCCBs, then switch to system recovery or backup protection operation according to the condition of CB_0. Moreover, the proposed methods of multiple DCCBs can be applied to all types of fully controlled modular DCCBs.

C. Coordination Method for Reclosing Process

The faulty line DCCB needs to reclose in 200–300 ms after a fault to distinguish a permanent fault or a temporary fault. The very basic reclosing method of DCCB is to totally reclose the main breaker subunits, then block all subunits again if the fault still exists, see Fig. 7(a). In the coordination control, the faulty line DCCB (CB_0) will control its current after being reclosed, and the i_{DC_ref} can be chosen as the pre-fault steady current. Therefore, if the fault disappears, the DC current can remain stable without the help of DCCB. If the subunits of DCCB are still inserted to control the DC current after a certain time delay, the fault can be considered as a permanent fault, and then the DCCB will be permanently blocked, see Fig. 7(b).

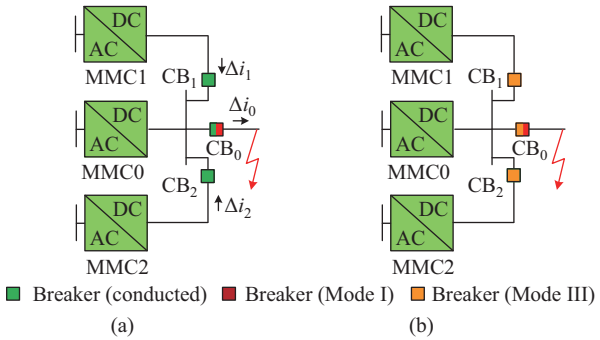

Fig. 7. Reclosing scheme of (a) conventional single DCCB; (b) multiple sequential DCCBs.

The reclosing process is divided into 3 steps, and its logic is shown in Fig. 8.

1) Before the reclosing command is received, the CB_0 is blocked. The $CB_{1\&2}$ continuously operates in the current-limiting mode.

2) When the reclosing command is sent to CB_0, it turns to current-limiting mode. If the fault exists, the faulty line current grows rapidly, and CB_0 will automatically limit the fault current. If the fault disappears, the power flow will gradually be rebalanced, and the current on the faulted line will not exceed the current limitation.

3) Based on the statement of CB_0, it will block again when the fault exists, or all CBs reclose their UFDs and LCSs after the fault disappears.

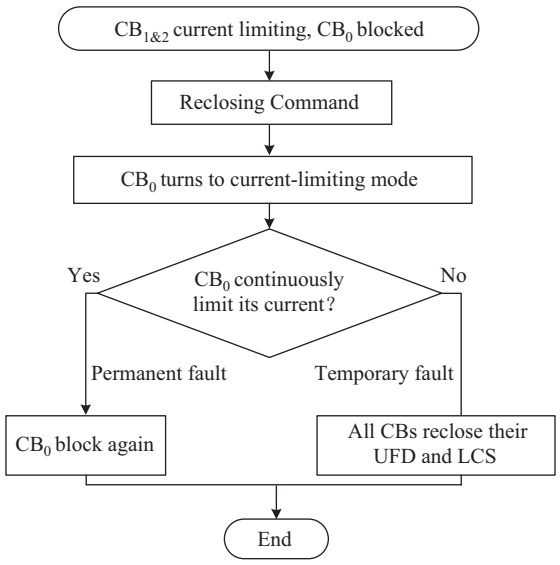

Fig. 8. Control logic of the reclosing process of multiple DCCBs.

IV. HVDC Grid Simulation Study

A. Simulation System

The superiority of the proposed coordination control is validated respectively in four- and seven-terminal 500 kV DC grids, aiming to showcase the applicability of the proposed method in a multilink HVDC grid. The simulation built in PSCAD V4.6 is based on the Zhangbei HVDC grid in China [26], [27], which is a four-terminal meshed DC grid (MMC 1&2&3&4). The additional three stations (MMC 5&6&7) are the phase II construction plan of this project, which will be built in the future.

The structure of the test system is shown in Fig. 9, in which the single-line diagram is used to represent a bipolar DC grid. All converters are controlled to zero reactive power, and the active power control parameters are also marked in Fig. 9. The parameters of each converter are given in Table I [28]. At $t =$ 1 s, a solid metal pole-to-pole DC short-circuit fault is applied at the near end of MMC1, and then the proposed coordination method is studied in the four- and seven-terminal DC grid.

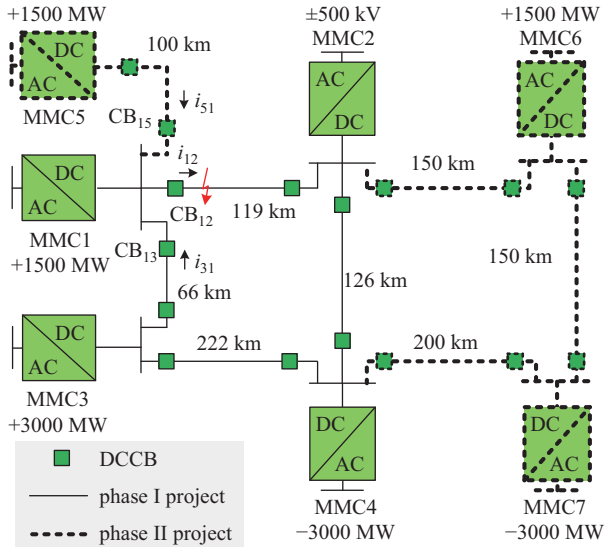

Fig. 9. Structure of the studied HVDC grid.

TABLE I
Parameters of the DC Grid

Items	Station1&2&5&6	Station 3&4&7
AC voltage	230 kV	500 kV
Transformer Capacity	1700 MW	3400 MW
Transformer Leakage	0.1 p.u.	0.15 p.u.
Arm Inductance	75 mH	100 mH
SM Number	250	250
SM Capacitance	7500 μF	15000 μF
L_{DC} Inductance	100 mH	100 mH

For the four-terminal DC grid (MMC 1–4), each DC bus is only linked to two transmission lines. Thus two DCCBs are used to handle the DC fault. When phase II of the project is commissioned, a seven-terminal DC grid is formed. Due to the lower impedance and higher energy storage in the seven-terminal system, the energy dissipation requirement is much higher than before. The DC bus connected to MMC 1&2&4 has 3 DC lines, then three DCCBs are used.

The studied DCCBs are the same as shown in Section II, which have 8 subunits in the simulation, and each one has a peak transient voltage of 100 kV. The DC fault is set at $t =$ 1.000 s and detected at $t =$ 1.003 s. The operation delay of the UFD is set as 2 ms. As all the DCCBs are deployed in the same station, the commutation delay, which is usually less than 100 μs, is neglected. Thus, all DCCBs can receive the control signal at the same time. For conventional DCCBs, the CB_{12} will be totally blocked at $t =$ 1.005 s, but the sequential DCCBs can start to insert their subunits from $t =$ 1.003 s.

Three cases are compared and discussed both in the four- and seven-terminal DC grid: 1) single conventional DCCB (Sin Con CB), 2) single sequential blocking DCCB (Sin Seq CB), and 3) coordination of multiple sequential DCCBs (Mul Seq CB). Case 3 will use a sequential current limiting DCCB (Mode III) on the adjacent lines to assist in the recovery of the DC grid. As indicated before, the single conventional DCCB is seen as the benchmarked case for comparison. The single sequential blocking DCCB has better performance than the conventional DCCB, and the proposed coordination control of multiple DCCBs will show a better performance than a single DCCB.

B. Coordination Protection in Four-terminal DC grid

1) Fault Interruption Performance of Primary Protection

The performance of coordination of a sequential DCCB is shown in Fig. 10, where the diagram of a single conventional DCCB is shown in a gray line for comparison. The single sequential blocking DCCB can reduce its peak current and fault energy. The simulation results show that the peak fault current is reduced from 15.9 kA to 12.9 kA, and the fault energy is reduced by 15.7%, see Fig. 10(a) and (b).

The coordination control of sequential DCCBs has a significant influence on the fault energy, although the peak fault current is reduced from 12.9 kA to 12.6 kA, the fault energy is reduced by 30.5% compared to the single conventional DCCB method. In Fig. 10(c), the adjacent line current i_{31} shows that

the fault current will decrease with the assistance of CB_{13}, and its fluctuation is limited by the DCCB current-limiting control during the recovery process. The e_{13} shows an energy dissipation of fault current interruption and current-limiting, see Fig. 10(d).

The system recovery speed is similar to the single conventional or sequential blocking DCCB, see Fig. 11(a). If multiple sequential DCCBs are used, the recovery process will be much faster. The active power of MMC1 will recover in approximately 35 ms after fault, which is reduced by around 20 ms compared to the single conventional DCCB. The capacitor voltage is also reduced from 2.6 kV to 2.36 kV, see Fig. 11(b), indicating that the proposed coordination method can result in a smaller fluctuation.

2) Fault Interruption Performance of Backup Protection

The coordination control can also reduce the energy dissipation on the backup DCCB (CB_{13}). The i_{31} and e_{13} under the conventional or sequential DCCB are shown in Fig. 12. As the conventional backup protection relies on the failure signal of faulty line DCCB, thus the MMC1 is blocked at 1.005 s, and CB_{13} are blocked 2 ms later. The CB_{13} is blocked at 1.005 s under the coordination methods of DCCBs, it will keep blocking after the failure of CB_{12}, and the MMC1 is blocked at 1.005 s.

The i_{31} and e_{13} of backup protection under single and coordination method of DCCB are shown in Fig. 12(a) and (b). The single sequential DCCB shows a better performance in backup protection than conventional DCCB, and the peak fault current and dissipated energy can be reduced by 25.4% and 29.2%, respectively. Due to an earlier blocking of DCCB, the coordination control of DCCBs has less peak fault current, and the fault energy on CB_{13} is reduced by 60.3%, which shows a lower energy loss and faster backup fault interruption. The dissipation energy is also reduced by 77.6%, which shows the system will lose less energy in the backup protection process.

C. Coordination Protection in Seven-terminal DC grid

1) Fault Interruption Performance of Primary Protection

The performance of coordination control of sequential DCCBs is shown in Fig. 13. The i_{12} drops to zero in 9.0 ms with multiple DCCBs, and the peak fault current is also reduced, see Fig. 13(a). The fault energy is reduced by 18.5% and 35.8%, if single or multiple sequential DCCBs are used, see Fig. 13(b). The fault current and energy on the adjacent line

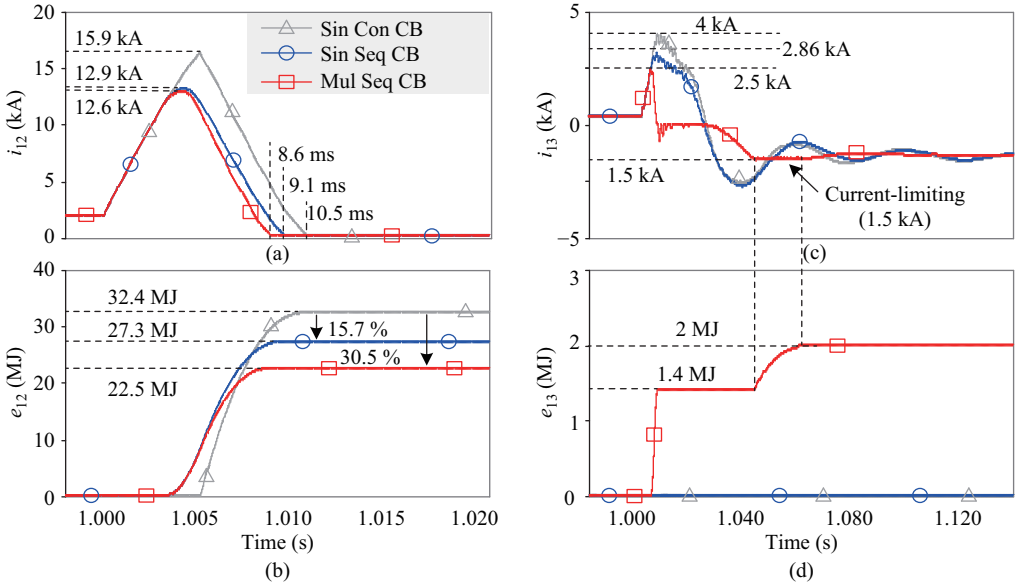

Fig. 10. Comparison of fault interruption performance of the single and multiple sequential DCCB. (a) Faulty line current. (b) Faulty line DCCB energy. (c) Adjacent line current. (d) Adjacent line DCCB energy.

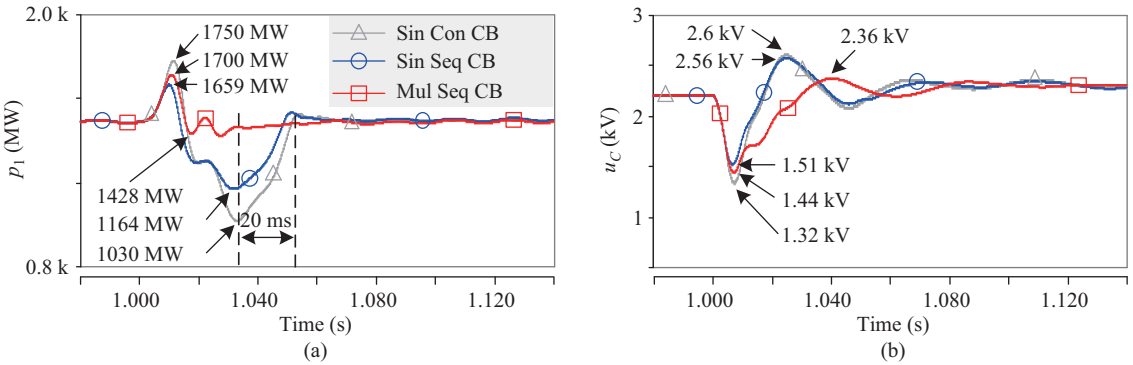

Fig. 11. Comparison of recovery process under sequential DCCB. (a) MMC1 output power. (b) MMC1 capacitor voltage.

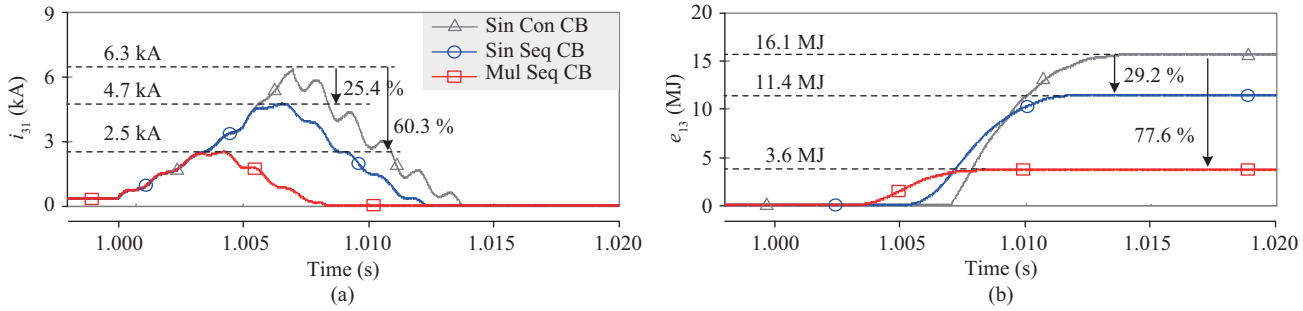

Fig. 12. Comparison of backup protection performance. (a) Adjacent line current. (b) Adjacent line CB's energy.

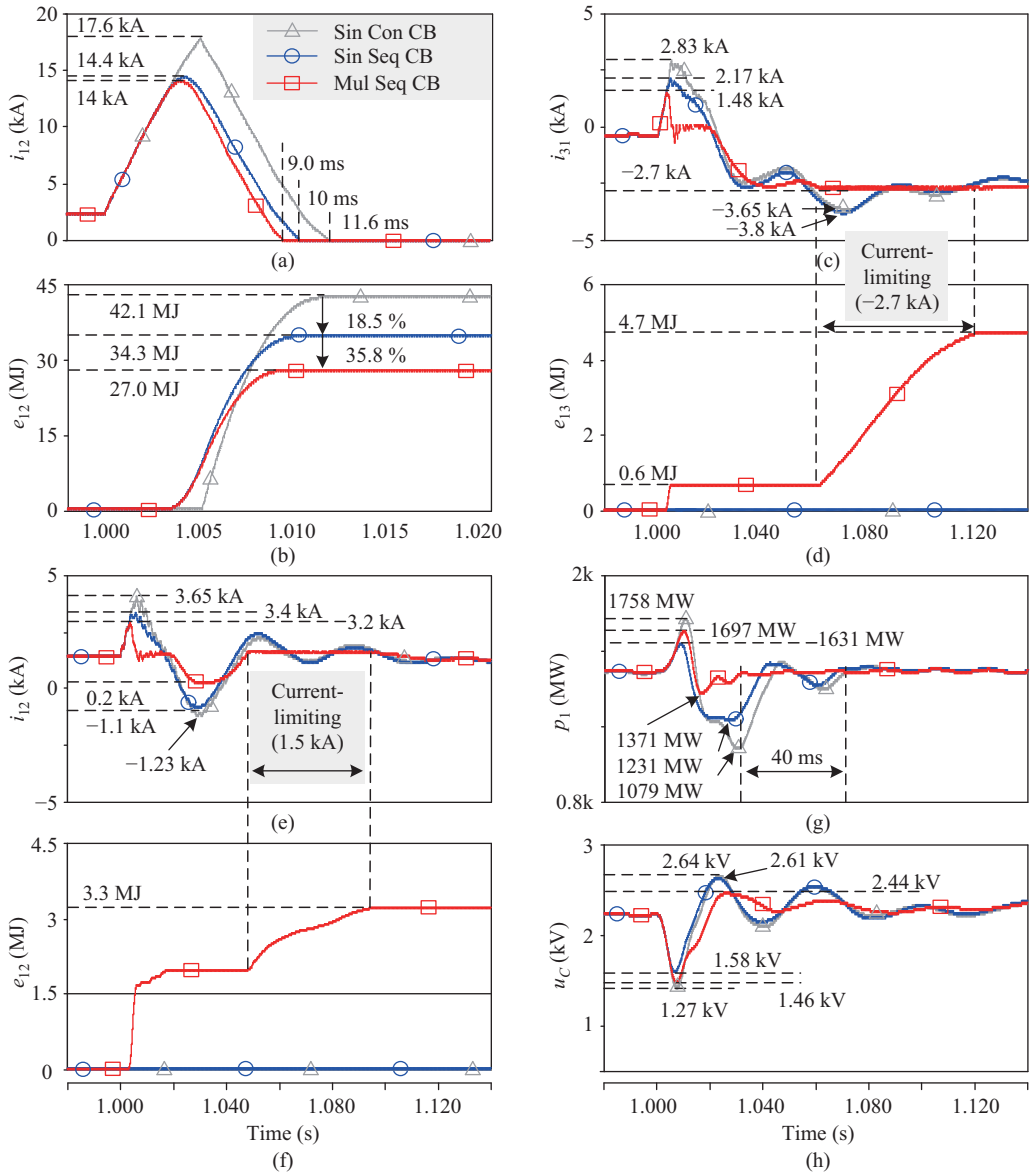

Fig. 13. Comparison of the fault interruption performance. (a) Faulty line current. (b) Faulty line DCCB energy. (c) Adjacent line31 current. (d) Adjacent line13 DCCB energy. (e) Adjacent line51 current. (f) Adjacent line15 DCCB energy. (g) MMC1 output power. (h) MMC1 capacitor voltages.

are shown in Fig. 13(c)–(f). The CB_{13} and CB_{15} both operate in the current-limiting mode, keeping i_{31} and i_{51} constant. As these two adjacent lines are not forced over the DC current reference, the fluctuation is reduced, and the system is restored faster.

The active power and average capacitor voltage of MMC1 are shown in Fig. 13(g)–(h). The coordination control results in a smaller fluctuation, and the system recovery time is reduced by around 40 ms compared to the single conventional DCCB case. If a comparison is made between Fig. 10, Fig. 11, and

Fig. 13, it is observed that the single DCCB seldom has an impact on the recovery process, but the proposed coordination method will significantly accelerate the process. Moreover, the proposed method shows a better performance in the seven-terminal DC grid, indicating that the proposed method is more suitable for future multi-link DC grid applications.

2) Fault Interruption Performance of Reclosing Protection

The pole-to-pole fault reclosing performance of the coordination method is verified in the seven-terminal system. The reclosing signal is given at $t = 1.3$ s. After a 2 ms relay delay, the second-time blocking signal is given to the faulty line DCCB.

As shown in Fig. 14(a), the peak fault current of the original reclosing method will increase to 7.3 kA within 2 ms. The current of the coordination method only reaches 2.5 kA because the CB_{12} is operating in the current limiting mode after being reclosed. The dissipated energy of CB_{12} will reach 51.5 MJ in the original method, but the energy is 29.9 MJ with the proposed coordination method, as shown in Fig. 14(b). It is noted that the dissipated energy of the coordination method is even less than the energy in the primary protection of a single conventional DCCB, and the total dissipated energy is further reduced by 41.9% when the reclosing process is considered.

According to the flow before reclosing, i_{13} will not reverse in such a short time. Thus, only CB_{15} can participate in the current limiting process. Therefore, only the current of CB_{15} is shown in Fig. 14(c). The current of the coordination control is limited to 1.5 kA, and the current will reach 2.5 kA without involving CB_{15}. Moreover, the current fluctuation of i_{51} is much smaller with the help of CB_{15}. The dissipated energy of CB_{15} only increases 0.4 MJ compared to the primary protection, as shown in Fig. 14(d). The results show that the coordination method can also reduce the peak current and dissipated energy in the reclosing process. The additional fault energy only increases a little, and the disturbance to the DC grid is much lower.

V. Economic Comparison and Discussion

The proposed method is compared to other DCCBs in protection performance, economic cost, and industrial feasibility. The comparison is between three types of DCCBs: 1) single conventional DCCB [10], 2) integrated DCCB [23], and 3) the proposed coordination of multiple sequential DCCBs.

The conventional DCCB uses one individual DCCB to protect each line, and the integrated DCCB uses one high-voltage valve to protect all connected lines. However, the conventional DCCB and integrated DCCB both totally block their main breaker after the current commutation process, so they have the same system fault response.

The coordination of multiple sequential DCCBs can achieve better protection performance by enhancing the controllability of the conventional DCCB. The proposed method can reduce the peak fault current, dissipated energy, and recovery times of the DC system, which is not discussed in the other methods. Taking the seven-terminal DC grid as an example, the three protection methods' fault responses are listed in Table II.

TABLE II
Fault Stress of Different DCCB

Protection methods	Sin Con DCCB	Integrated DCCB	Mul Seq DCCB
primary peak current (kA)	17.6	17.6	14
primary fault energy (MJ)	42.1	42.1	27
secondary peak current (kA)	7.3	7.3	2.5
secondary fault energy (MJ)	44.5	44.5	29.9
recovery time (ms)	75	75	35

The proposed method can limit the fault current and dissipated energy during the fault, which means the system will suffer less disturbance, and the cost of one DCCB will

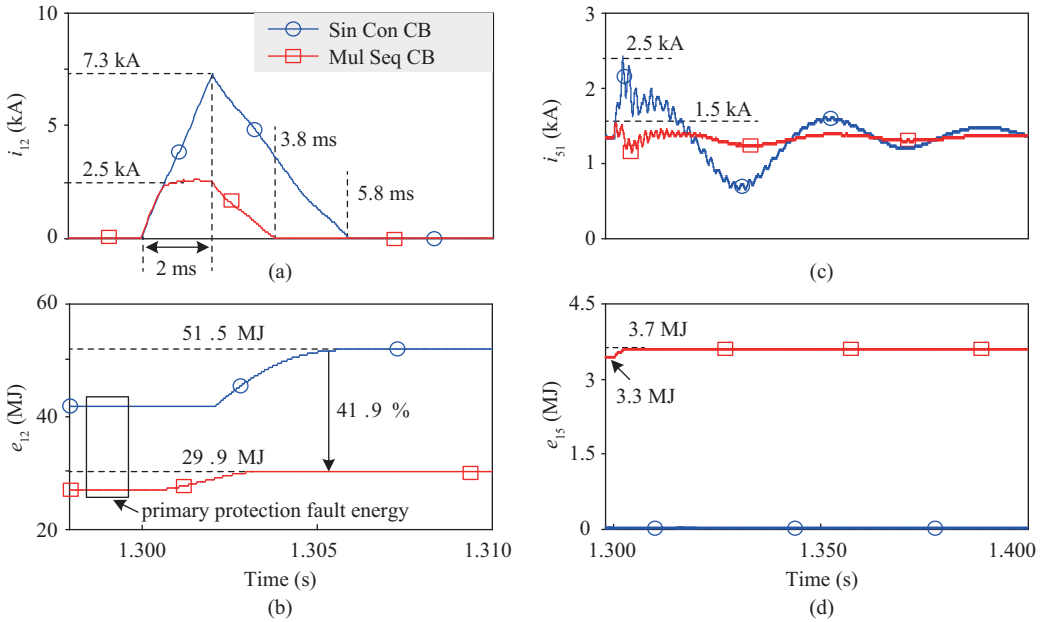

Fig. 14. Comparison of reclosing performance of the single conventional DCCB and multiple sequential DCCBs. (a) Faulty line current. (b) Faulty line DCCB energy. (c) Adjacent line current. (d) Adjacent line DCCB energy.

be reduced. The requirements for the IGBTs under different protection methods are discussed. IGBTs can achieve a high turnoff current by applying high gate-emitter voltage. It will be primarily threatened by overheating when turning off a large current, and the IGBT's junction temperature (T_{vj}) can be calculated by its power loss and thermal module [29]. Taking the conventional protection method or coordination method in the seven-terminal DC grid as an example (Fig. 13(a)), the junction temperature of ABB's 4.5 kV/3 kA IGBT [30] and 4.5 kV/2 kA IGBT [31] are compared, as shown in Fig. 15.

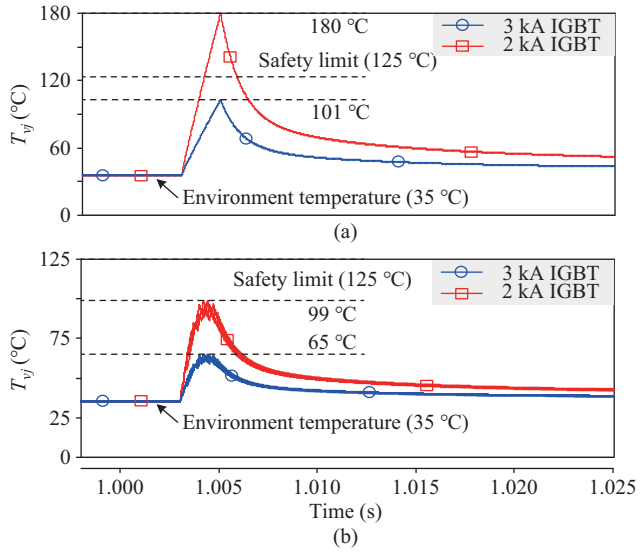

Fig. 15. Junction Temperature of main breaker IGBTs under (a) single conventional DCCB, (b) coordination method of multiple sequential DCCBs.

In the conventional method, a 3 kA IGBT can turn off a 17.6 kA fault current when its junction temperature reaches 101°C, but a 2 kA IGBT will reach 180°C, see Fig. 15(a). The temperature of a 2 kA IGBT will exceed the safety limit of 125°C, so it is not satisfied in the conventional protection method. In the coordination method, the junction temperature reaches 65°C for a 3 kA IGBT, and the temperature of 8 sub-units of a 2 kA IGBT reaches 99°C, respectively. Therefore, the 2 kA IGBT can satisfy the protection requirements, and the 3 kA IGBT is unnecessary.

The proposed coordination method can reduce the requirements for large current IGBTs, but the cost of an integrated DCCB is the cheapest as it only uses one high-voltage valve to protect multiple lines. However, it also has some drawbacks compared to individual DCCBs. The integrated DCCB relies on many LCSs and UFDs to ensure the fault current on every line flows through one high-voltage valve, but individual DCCBs have their own corresponding LCS and UFD. The UFDs and LCSs used are shown in Table III, in which n is the number of lines connected to the DC bus.

The integrated DCCB needs more LCSs and UFDs in one breaker, and half of the LCSs and UFDs are used to build the commutation circuit during fault. The single DCCB method only triggers the faulty line DCCB to isolate the fault, and the proposed coordination method will trigger all nearby DCCBs. However, the integrated DCCB needs a complex

TABLE III
ECONOMIC EFFICIENCY COMPARISON

Protection methods	Sin Con DCCB	Integrated DCCB	Mul Seq DCCB
Number of DCCB	n	1	n
Number of UFDs and LCSs	n	$2n+2$	n
Triggered number of UFDs and LCSs during one fault	1	$n+1$	n
Near backup protection?	yes	no	yes

structure design to connect multiple lines in one DCCB, but the individual DCCB only needs one input and one output line. The success of integrated DCCB relies on every UFD and LCS's acerate operation, and it lacks near-end backup protection capability. The proposed coordination method has a simple current commutation process for each DCCB, and the nearby DCCBs can achieve backup protection.

The coordination method of DCCB can be achieved by software upgrades from the existing single DCCBs. The IGBT's control board can already measure current and voltage on every sub-module, but the signal interconnection between DCCBs needs more devices. When the proposed method is upgraded from the existing DCCBs, it will have more reliability than the integrated DCCB. The system still has enough capability for backup protection even if one DCCB fails.

VI. CONCLUSION

In this paper, coordination methods of multiple DCCBs are proposed to protect the HVDC grid; the fault energy is shared, and the system recovery speed is increased. The control methods for primary/backup protection and reclosing logic are discussed. The coordination of sequential DCCBs is preferred due to the fact it has better controllability than single DCCBs.

The proposed coordination method enhanced the controllability of multiple DCCBs, so the effect will be better than single DCCB protection, and it is verified in the Zhangbei system. For example, the energy dissipation requirement is reduced by 30.5–41.9%, and the fault recovery time is reduced by 20–40 ms. Compared with a four-terminal DC grid, the proposed method achieves better results in a seven-terminal DC grid. This indicates that the proposed method has better applicability for an HVDC grid with more links connected to one DC bus.

The proposed method's effect relies on the correct operation of all DCCBs; a failure operation of one certain DCCB may cause a reduction in the protection effect of the proposed method. The trigger signal transmission from the faulty line DCCB to adjacent DCCBs also impacts the protection effect; a fast and reliable signal transmission is needed to activate proper coordination protection.

It should also be highlighted that an experimental validation of the proposed protection scheme, although highly desirable to verify its performance, falls out of the scope of this study. However, the experimental verification of the single sequential DCCB has been shown in [19]. Therefore, a better protection performance of multiple DCCBs can be expected in the meshed DC grid.

REFERENCES

[1] N. Flourentzou, V. G. Agelidis, and G. D. Demetriades, "VSC-based HVDC power transmission systems: an overview," *IEEE Transactions on Power Electronics*, vol. 24, no. 3, pp. 592–602, Mar. 2009.

[2] D. Van Hertem and M. Ghandhari, "Multi-terminal VSC HVDC for the European supergrid: obstacles," *Renewable and Sustainable Energy Reviews*, vol. 14, no. 9, pp. 3156–3163, Dec. 2010.

[3] T. An, G. F. Tang, and W. N. Wang, "Research and application on multi-terminal and DC grids based on VSC-HVDC technology in China," *High Voltage*, vol. 2, no. 1, pp. 1–10, Mar. 2017.

[4] X. Han, W. X. Sima, M. Yang, L. C. Li, T. Yuan, and Y. Si, "Transient characteristics Under Ground and short-circuit faults in a ±500 kV MMC-based HVDC system with hybrid DC circuit breakers," *IEEE Transactions on Power Delivery*, vol. 33, no. 3, pp. 1378–1387, Jun. 2018.

[5] S. Li, J. Z. Xu, Y. Lu, C. Y. Zhao, J. Y. Zhang, C. X. Jiang, and S. M. Qiu, "An auxiliary DC circuit breaker utilizing an augmented MMC," *IEEE Transactions on Power Delivery*, vol. 34, no. 2, pp. 561–571, Apr. 2019.

[6] J. Z. Xu, X. B. Zhao, H. Jing, J. Liang, and C. Y. Zhao, "DC fault current clearance at the source side of HVDC grid using hybrid MMC," *IEEE Transactions on Power Delivery*, vol. 35, no. 1, pp. 140–149, Feb. 2020.

[7] W. X. Lin, D. Jovcic, S. Nguefeu, and H. Saad, "Full-bridge MMC converter optimal design to HVDC operational requirements," *IEEE Transactions on Power Delivery*, vol. 31, no. 3, pp. 1342–1350, Jun. 2016.

[8] Q. Song, R. Zeng, Z. Q. Yu, W. H. Liu, Y. L. Huang, W. B. Yang, and X. Q. Li, "A modular multilevel converter integrated with DC circuit breaker," *IEEE Transactions on Power Delivery*, vol. 33, no. 5, pp. 2502–2512, Oct. 2018.

[9] S. Wang, C. Y. Li, O. D. Adeuyi, G. Li, C. E. Ugalde-Loo, and J. Liang, "Coordination of MMCs with hybrid DC circuit breakers for HVDC grid protection," *IEEE Transactions on Power Delivery*, vol. 34, no. 1, pp. 11–22, Feb. 2019.

[10] A. Hassanpoor, J. Häfner, and B. Jacobson, "Technical assessment of load commutation switch in hybrid HVDC breaker," *IEEE Transactions on Power Electronics*, vol. 30, no. 10, pp. 5393–5400, Oct. 2015.

[11] G. F. Tang, Z. Y. He, H. Pang, X. M. Huang, and X. P. Zhang, "Basic topology and key devices of the five-terminal DC grid," *CSEE Journal of Power and Energy Systems*, vol. 1, no. 2, pp. 22–35, Jun. 2015.

[12] H. Pang and X. G. Wei, "Research on key technology and equipment for Zhangbei 500kV DC grid," in *2018 International Power Electronics Conference (IPEC)*, Niigata, 2018, pp. 2343–2351.

[13] D. Jovcic, G. F. Tang, and H. Pang, "Adopting circuit breakers for high-voltage DC networks: appropriating the vast advantages of DC transmission grids," *IEEE Power and Energy Magazine*, vol. 17, no. 3, pp. 82–93, May/Jun. 2019.

[14] R. Majumder, S. Auddy, B. Berggren, G. Velotto, P. Barupati, and T. U. Jonsson, "An alternative method to build DC switchyard with hybrid DC breaker for DC grid," *IEEE Transactions on Power Delivery*, vol. 32, no. 2, pp. 713–722, Apr. 2017.

[15] B. Li, J. W. He, Y. Li, W. J. Wen, and B. T. Li, "A novel current-commutation-based FCL for the flexible DC grid," *IEEE Transactions on Power Electronics*, vol. 35, no. 1, pp. 591–606, Jan. 2020.

[16] Y. X. Guo, G. Wang, D. H. Zeng, H. F. Li, and H. Chao, "A thyristor full-bridge-based DC circuit breaker," *IEEE Transactions on Power Electronics*, vol. 35, no. 1, pp. 1111–1123, Jan. 2020.

[17] A. Jamshidi Far and D. Jovcic, "Design, modeling and control of hybrid DC circuit breaker based on fast thyristors," *IEEE Transactions on Power Delivery*, vol. 33, no. 2, pp. 919–927, Apr. 2018.

[18] Y. Song, J. F. Sun, M. Saeedifard, S. C. Ji, L. Y. Zhu, A. P. S. Meliopoulos, and L. Graber, "Reducing the fault-transient magnitudes in multiterminal HVDC grids by sequential tripping of hybrid circuit breaker modules," *IEEE Transactions on Industrial Electronics*, vol. 66, no. 9, pp. 7290–7299, Sep. 2019.

[19] M. H. Hedayati and D. Jovcic, "Reducing peak current and energy dissipation in hybrid HVDC CBs using disconnector voltage control," *IEEE Transactions on Power Delivery*, vol. 33, no. 4, pp. 2030–2038, Aug. 2018.

[20] G. R. Liu, F. Xu, Z. Xu, Z. R. Zhang, and G. Tang, "Assembly HVDC breaker for HVDC grids with modular multilevel converters," *IEEE Transactions on Power Electronics*, vol. 32, no. 2, pp. 931–941, Feb. 2017.

[21] C. Y. Li, J. Liang, and S. Wang, "Interlink hybrid DC circuit breaker," *IEEE Transactions on Industrial Electronics*, vol. 65, no. 11, pp. 8677–8686, Nov. 2018.

[22] A. Mokhberdoran, D. Van Hertem, N. Silva, H. Leite, and A. Carvalho, "Multiport hybrid HVDC circuit breaker," *IEEE Transactions on Industrial Electronics*, vol. 65, no. 1, pp. 309–320, Jan. 2018.

[23] E. Kontos, T. Schultz, L. Mackay, L. M. Ramirez-Elizondo, C. M. Franck, and P. Bauer, "Multiline breaker for HVdc applications," *IEEE Transactions on Power Delivery*, vol. 33, no. 3, pp. 1469–1478, Jun. 2018.

[24] W. X. Lin, D. Jovcic, S. Nguefeu, and H. Saad, "Modelling of high-power hybrid DC circuit breaker for grid-level studies," *IET Power Electronics*, vol. 9, no. 2, pp. 237–246, Feb. 2016.

[25] C. Y. Li, C. Y. Zhao, J. Z. Xu, Y. K. Ji, F. Zhang, and T. An, "A pole-to-pole short-circuit fault current calculation method for DC grids," *IEEE Transactions on Power Systems*, vol. 32, no. 6, pp. 4943–4953, Nov. 2017.

[26] X. S. Guo, Y. Zhou, N. Mei, and Y. Lu, "Research on the fault current characteristic and suppression strategy of Zhangbei project," *Proceedings of the CSEE*, vol. 38, no. 18, pp. 5438–5446, Sep. 2018.

[27] X. B. Zhao, J. P. Ding, J. Z. Xu and J. S. Yuan, "Hybrid MMC with Low Voltage Operations and DC Fault Ride-through Capabilities Based on Auxiliary Full-bridge Converter," *CSEE Journal of Power and Energy Systems*, vol. 8, no. 3, pp. 864–871, May 2022.

[28] Y. Q. Wang, K. G. Wang, G. Li, F. J. Wu, K. W. Wang and J. Liang, "Generalized Switched-Capacitor Step-up Multilevel Inverter Employing Single DC Source," in *CSEE Journal of Power and Energy Systems*, vol. 8, no. 2, pp. 439–451, Mar. 2022.

[29] X. B. Zhao, L. X. Chen, G. Li, J. Z. Xu and J. S. Yuan, "Coordination Method for DC Fault Current Suppression and Clearance in DC Grids," *CSEE Journal of Power and Energy Systems*, vol. 8, no. 5, pp. 1438–1447, Sep. 2022.

[30] ABB. (2017, Nov.). 5SNA 3000K452300 data sheet. [Online]. Available: https://www.darrahelectric.com/media/documents/5SNA%203000K452300%20Data%20Sheet.pdf.

[31] ABB. (2016, Oct.). 5SNA 2000K452300 data sheet. [Online]. Available: https://library.e.abb.com/public/9a567b346e2e46428a5a249c4206715b/5SNA%202000K452300%205SYA%201441-01%2010-2016.pdf.

Xibei Zhao received a Ph.D. degree in Electrical Engineering and Its Automation from North China Electric Power University in 2021. He is currently a lector at NCEPU since August 2022. His research interests include HVDC grid operation and protection.

Jianzhong Xu (M'14) received a Ph.D. degree in Electrical Engineering from North China Electric Power University, Beijing, China, in 2014. He is currently an Associate Professor with the State Key Laboratory of Alternate Electrical Power System with Renewable Energy Sources, NCEPU, China. His research interests include the high-speed electromagnetic transient modeling, control, and protection of MMC-HVDC and DC grids.

Gen Li (M'18) received a Ph.D. degree in Electrical Engineering from Cardiff University, Cardiff, U.K., in 2018. He is currently a Professor with Technical University of Denmark, Denmark. His research interests include control and protection of HVDC and MVDC technologies, power electronics, reliability modeling and evaluation of power electronics systems.

Jinsha Yuan received a Ph.D. degree in Electrical Engineering and Its Automation from North China Electric Power College, Baoding, China, in 1992. He is currently a Professor and a Ph.D. Supervisor with North China Electric Power University, Baoding. His research interests include intelligent information processing technology, wireless communication, and electromagnetic field numerical calculation method and application.

Jun Liang received a Ph.D. degree from the China Electric Power Research Institute (CEPRI), Beijing, in 1998. Currently, he is a Professor at the School of Engineering, Cardiff University, Cardiff, U.K. His research interests include HVDC, MVDC, FACTS, power system stability control, power electronics, and renewable power generation.